

Density Functional Theory Studies on Copper Phenanthroline Complexes

Arturo Robertazzi,[†] Alessandra Magistrato,^{*†} Paul de Hoog,[‡] Paolo Carloni,[†] and Jan Reedijk[‡]

International School for Advanced Studies and CNR-INFM-Democritos National Simulation Center, Trieste, Italy, and Leiden Institute of Chemistry, Gorlaeus Laboratories, Leiden University, P.O. Box 9502, 2300 RA Leiden, The Netherlands

Received October 2, 2006

Density functional theory calculations have been employed to investigate the role of structural properties of copper phenanthroline complexes for DNA-cleavage activity. Structural changes imposed on the coordination geometries of $\text{Cu}(\text{phen})_2^{2+}$ (phen = 1,10-phenanthroline) linked by a serinol bridge (abbreviated as Clip) were studied, as well as their energetic profiles. Our calculations show that structures of these copper complexes (in this work named as clipped complexes) strongly depend on the position of the link, rather than on the copper oxidation state. Ionization energies slightly differ among the three selected complexes, while inner-sphere reorganization energies more markedly depend on the serinol link. However, the relative rates of the redox reaction of $\text{Cu}(\text{phen})_2$, $\text{Cu}(2\text{-Clip-phen})$, and $\text{Cu}(3\text{-Clip-phen})$ were found not to correlate with their relative DNA-cleavage activity experimentally observed. Thus, the serinol link mainly affects the structural properties of copper phenanthroline complexes rather than their electronic properties. Docking simulations of clipped and nonclipped $\text{Cu}(\text{I})$ phenanthroline complexes on a DNA 16mer, $d[\text{CGCTCAACTGTGATAC}]_2$, were finally performed to assess how different structural properties could affect the formation of DNA adducts. This analysis revealed that the most stable adducts of $\text{Cu}(\text{phen})_2^{2+}$ and $\text{Cu}(3\text{-Clip-phen})^+$ with DNA bind in the minor groove, whereas $\text{Cu}(2\text{-Clip-phen})^+$ binds preferentially into the major groove.

Introduction

Copper complexes of 1,10-phenanthroline (phen) and their derivatives are widely used chemical nucleases employed as footprinting reagents for determining ligand binding sites and recently also for therapeutic use.^{1,2} These compounds, along with Fe, Mn complexes, and bleomycin,³ cut DNA at physiological conditions.⁴ The cleavage activity of the best-studied complex, $\text{Cu}(\text{phen})_2$, which is significantly more reactive than the monophen complexes, $\text{Cu}(\text{phen})$,^{1,5–17}

supposedly occurs according to the following mechanism (see Scheme 1):^{3,18} (a) $\text{Cu}(\text{phen})_2^{2+}$ is reduced in solution to $\text{Cu}(\text{phen})_2^+$; (b) $\text{Cu}(\text{phen})_2^+$ binds DNA noncoordinatively; (c)

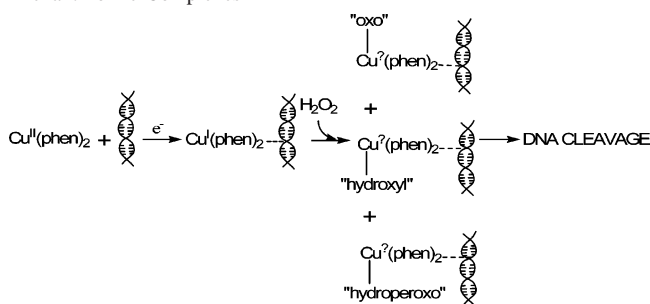
* To whom correspondence should be addressed. E-mail: alema@sissa.it.

[†] International School for Advanced Studies and CNR-INFM-Democritos National Simulation Center.

[‡] Leiden University.

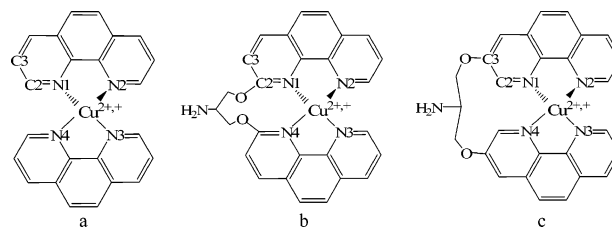
- (1) Sigman, D. S.; Mazumder, A.; Perrin, D. M. *Chem. Rev.* **1993**, *93*, 2295–2316.
- (2) Pitié, M.; Croisy, A.; Carrez, D.; Boldron, C.; Meunier, B. *ChemBioChem* **2005**, *6*, 686–691.
- (3) Pitié, M.; Boldron, C.; Pratiel, G. *Adv. Inorg. Chem.* **2006**, *58*, 77–130.
- (4) Sigman, D. S.; Graham, D. R.; Daurora, V.; Stern, A. M. *J. Biol. Chem.* **1979**, *254*, 2269–2272.
- (5) Chen, T.; Greenberg, M. M. *J. Am. Chem. Soc.* **1998**, *120*, 3815–3816.

- (6) Kalsani, V.; Schmittel, M.; Listorti, A.; Accorsi, G.; Armaroli, N. *Inorg. Chem.* **2006**, *45*, 2061–2067.
- (7) Miller, M. T.; Gantzel, P. K.; Karpishin, T. B. *Inorg. Chem.* **1998**, *37*, 2285–2290.
- (8) Hirohama, T.; Kuranuki, Y.; Ebina, E.; Sugizaki, T.; Arii, H.; Chikira, M.; Tamil Selvi, P.; Palaniandavar, M. *J. Inorg. Biochem.* **2005**, *99*, 1205–1219.
- (9) Thomas, A. M.; Nethaji, M.; Mahadevan, S.; Chakravarty, A. R. *J. Inorg. Biochem.* **2003**, *94*, 171–178.
- (10) Meijler, M. M.; Zelenko, O.; Sigman, D. S. *J. Am. Chem. Soc.* **1997**, *119*, 1135–1136.
- (11) Oyoshi, T.; Sugiyama, H. *J. Am. Chem. Soc.* **2000**, *122*, 6313–6314.
- (12) Chikira, M.; Tomizawa, Y.; Fukita, D.; Sugizaki, T.; Sugawara, N.; Yamazaki, T.; Sasano, A.; Shindo, H.; Palaniandavar, M.; Antholine, W. E. *J. Inorg. Biochem.* **2002**, *89*, 163–173.
- (13) Lu, L.-P.; Zhu, M.-L.; Yang, P. *J. Inorg. Biochem.* **2003**, *95*, 31–36.
- (14) Sigman, D. S. *Acc. Chem. Res.* **1986**, *19*, 180–186.
- (15) Pratiel, G.; Bernardou, J.; Meunier, B. *Angew. Chem., Int. Ed.* **1995**, *34*, 746–769.
- (16) Pogozelski, W. K.; Tullius, T. D. *Chem. Rev.* **1998**, *98*, 1089–1107.
- (17) Chen, C. H. B.; Milne, L.; Landgraf, R.; Perrin, D. M.; Sigman, D. S. *ChemBioChem* **2001**, *2*, 735–740.
- (18) Thederahn, T. B.; Kuwabara, M. D.; Larsen, T. A.; Sigman, D. S. *J. Am. Chem. Soc.* **1989**, *111*, 4941–4946.

Scheme 1. Putative DNA-Cleavage Mechanism of Copper Phenanthroline Complexes^a

$\text{Cu}(\text{phen})_2^+$ is oxidized to $\text{Cu}(\text{phen})_2^{2+}$ by H_2O_2 produced in loco via redox reactions; (d) upon oxidation, the metal ion gains one ligand,¹⁹ leading to Cu-“oxo” and/or Cu-“hydroxyl” species, the exact nature of which is still unknown;³ (e) an oxidative attack mediated by these copper compounds leads to DNA cleavage mainly at C-1', C-4', or C-5' of the 2-deoxyribose units.^{10,11,20–22}

Unfortunately, the use of $\text{Cu}(\text{phen})_2$ presents some drawbacks that limit its applicability. Indeed, its formation is rather unfavorable under physiological conditions because of the very small association constant of the second phenanthroline.^{23,24} Moreover, $\text{Cu}(\text{phen})_2$ shows a small DNA sequence selectivity, although it is not nucleotide specific.^{25,26} In an effort to overcome these drawbacks, Pitié et al.³ used a serinol bridge (abbreviated as Clip) to link two phenanthroline ligands on positions 2 (resulting in $\text{Cu}(\text{2-Clip-phen})$) and 3 (resulting in $\text{Cu}(\text{3-Clip-phen})$) (Figure 1). These chemical modifications lead to several advantages. First, the link ensures that the two phen ligands both coordinate to Cu. Second, $\text{Cu}(\text{2-Clip-phen})$ and $\text{Cu}(\text{3-Clip-phen})$ complexes turn out to cleave DNA macromolecules 2 and 60 times more efficiently than $\text{Cu}(\text{phen})_2$, respectively, but with a mechanism similar to that of $\text{Cu}(\text{phen})_2$.^{3,27,28} The reason for this increase in DNA-cleavage activity is not completely clear, but it is supposed to arise from structural characteristics rather than from electronic properties.²⁹ Indeed, no correlation was found between the redox properties and the DNA-cleavage efficiency of clipped and non-clipped complexes. Finally, the presence of the serinol bridge allows one to functionalize copper phenanthroline compounds with sequence specific anticancer drugs, rendering

**Figure 1.** Structure and labeling scheme of $\text{Cu}(\text{phen})_2^{2+}$ (a), $\text{Cu}(\text{2-Clip-phen})^{2+}$ (b), and $\text{Cu}(\text{3-Clip-phen})^{2+}$ (c).

the compound highly sequence selective and possibly even providing it with anticancer properties. In this respect, examples include a conjugate of 3-Clip-phen with (i) an analogue of distamycin, which showed promising results toward a selective binding to DNA;^{22,30–32} and (ii) cisplatin derivatives, with the platinum units playing two roles, namely, as an antitumor drug and as an anchor to DNA.³³

Despite the promising role of these clipped derivatives, modeling studies^{34,35} and quantum chemical calculations^{36–41} have been reported only for free copper phenanthroline complexes. Modeling studies,³⁴ corroborated by classical simulations,³⁵ suggest that the “noncovalent” binding of $\text{Cu}(\text{phen})_2^+$ to double-strand (ds) DNA involves minor-groove binding of one phen and partial intercalation of the other. Quantum chemical studies, instead, have mainly focused on the structural and spectroscopic properties of $\text{Cu}(\text{phen})_2$ and its derivatives, such as $\text{Cu}(\text{dmp})_2$, $[\text{Cu}(\text{phen})(\text{PPh}_3)_2]$, etc.^{36–41}

In the present work, we have carried out an extensive Density Functional Theory (DFT) study of the structural and electronic properties of $\text{Cu}(\text{2-Clip-phen})$ and $\text{Cu}(\text{3-Clip-phen})$ in $\text{Cu}(\text{II})$ and $\text{Cu}(\text{I})$ oxidation states, comparing them to those of free $\text{Cu}(\text{phen})_2$ complexes. The study was complemented by using docking calculations of copper phenanthroline compounds to ds DNA. Similarities and differences are pointed out, aiming at rationalizing their relative efficiency in DNA cleavage. This study may help in developing rationally engineered DNA cleavers in which sequence-specific anticancer drugs are combined with copper phenanthroline complexes.^{3,33}

Computational Details

All DFT calculations were performed using *Gaussian03*.⁴² Geometry optimizations were carried out without symmetry con-

- (19) Nakai, H.; Deguchi, Y. *Bull. Chem. Soc. Jpn.* **1975**, *48*, 2557–2560.
 (20) Goynes, T. E.; Sigman, D. S. *J. Am. Chem. Soc.* **1987**, *109*, 2846–2848.
 (21) Kuwabara, M.; Yoon, C.; Goynes, T.; Thederahn, T.; Sigman, D. S. *Biochemistry* **1986**, *25*, 7401–7408.
 (22) Pitié, M.; Burrows, C. J.; Meunier, B. *Nucl. Acids Res.* **2000**, *28*, 4856–4864.
 (23) James, B. R.; Williams, R. J. P. *J. Chem. Soc.* **1961**, 2007.
 (24) Sillen, L. G.; Martell, A. E. *Stability Constants of Metal-Ion Complexes*; The Chemical Society of London: Oxford, 1971.
 (25) Veal, J. M.; Rill, R. L. *Biochemistry* **1988**, *27*, 1822–1827.
 (26) Yoon, C.; Kuwabara, M. D.; Law, R.; Wall, R.; Sigman, D. S. *J. Biol. Chem.* **1988**, *263*, 8458–8463.
 (27) Pitié, M.; Sudres, B.; Meunier, B. *Chem. Commun.* **1998**, 2597–2598.
 (28) Pitié, M.; Donnadiou, B.; Meunier, B. *Inorg. Chem.* **1998**, *37*, 3486–3489.
 (29) Pitié, M.; Boldron, C.; Gornitzka, H.; Hemmert, C.; Donnadiou, B.; Meunier, B. *Eur. J. Inorg. Chem.* **2003**, 528–540.

- (30) Pitié, M.; Van Horn, J. D.; Brion, D.; Burrows, C. J.; Meunier, B. *Bioconjugate Chem.* **2000**, *11*, 892–900.
 (31) Bales, B. C.; Kodama, T.; Weledji, Y. N.; Pitié, M.; Meunier, B.; Greenberg, M. M. *Nucleic Acids Res.* **2005**, *33*, 5371–5379.
 (32) Pitié, M.; Meunier, B. *Bioconjugate Chem.* **1998**, *9*, 604–611.
 (33) de Hoog, P.; Boldron, C.; Gamez, P.; Sliedregt-Bol, K.; Roland, I.; Pitié, M.; Kiss, R.; Meunier, B.; Reedijk, J. *J. Med. Chem.* **2007**, in press.
 (34) Stockert, J. C. *J. Theor. Biol.* **1989**, *137*, 107–111.
 (35) Hermann, T.; Heumann, H. *RNA* **1995**, *1*, 1009–1017.
 (36) Howell, S. L.; Gordon, K. C. *J. Phys. Chem. A* **2004**, *108*, 2536–2544.
 (37) Philip Coppens, I. V. N. *Int. J. Quantum Chem.* **2005**, *101*, 611–623.
 (38) Chen, L. X.; Shaw, G. B.; Novozhilova, I.; Liu, T.; Jennings, G.; Attenkofer, K.; Meyer, G. J.; Coppens, P. *J. Am. Chem. Soc.* **2003**, *125*, 7022–7034.
 (39) Siddique, Z. A.; Yamamoto, Y.; Ohno, T.; Nozaki, K. *Inorg. Chem.* **2003**, *42*, 6366–6378.
 (40) Zgierski, M. Z. *J. Chem. Phys.* **2003**, *118*, 4045–4051.
 (41) Osako, T.; Nagatomo, S.; Kitagawa, T.; Cramer, C.; Itoh, S. *J. Biol. Inorg. Chem.* **2005**, *10*, 581–590.

straints at the BLYP^{43,44} level using the 6-31G(d) basis set on C, H, O, and N atoms and the SDD⁴⁵ basis set and effective core potential (ECP) on Cu (as implemented in *Gaussian03*, SDD is D95V up to Ar and Stuttgart/Dresden ECPs for the remaining elements of the periodic table). Harmonic frequency calculations were performed to confirm that the calculated structures were minima. After optimization, single-point calculations were performed, adding one polarization function on hydrogen and one diffuse function on heavy atoms (6-31+G(d,p)), to calculate electron densities and estimate solvent effects with the polarizable continuum model (PCM)⁴⁶ (water solvent, $\epsilon = 78.39$ as implemented in *Gaussian03*). The B3LYP^{44,47} functional with a range of basis sets (6-31G(d), 6-31+G(d,p), 6-311++G(d,p)) was also used to test the geometrical dependence on the exchange-correlation functional. Moreover, calculations with an even larger basis set (6-311++G(2d,2p)) were performed to test the energy dependence on the number of basis functions. In addition, test calculations showed that the basis set superposition error (BSSE, estimated using Boys and Bernardi's counterpoise method)⁴⁸ is as small as 5% of the overall binding energies reported in Table 3.

Open-shell Cu(II) complexes were treated with a spin-unrestricted formalism. A detailed analysis of the spin densities has been carried out for all the Cu(II) complexes studied in this work to check if unrealistic localization of the unpaired electron occurs. As reported previously,⁴⁹ DFT calculations may give an unphysical localization of the spin densities due to the self-interaction error. However, few cases in which good agreement is observed between DFT (BLYP, B3LYP) calculations and experimental data were reported in the literature.^{50–52} Calculations with both BLYP and B3LYP were performed on our systems. As expected,⁵³ the B3LYP functional provides more feasible spin densities compared with the BLYP functional, but differences between the two exchange correlation functionals are virtually constant for the three complexes. Therefore, if a small overstabilization of the oxidized copper energies occurred, clipped and unclipped species would be similarly affected, influencing the absolute value of ionization energies to a similar extent

and confirming the observed relative trends. Indeed, energy and geometry trends estimated with the BLYP, B3LYP, BP,^{43,54} and PW91⁵⁵ functionals hardly differ (see Discussion and Supporting Information). To further support this point, additional post-HF MP2⁵⁶ calculations (which are not affected by the self-interaction error) were performed on clipped and unclipped water-coordinated copper phenanthroline complexes, showing that although at the MP2 level the unpaired electron is properly localized on Cu(II), ionization energies have a very similar trend to those of DFT calculations.

Bonding interactions were characterized using Bader et al.'s theory of atoms in molecules (AIM),^{57–59} which partitions molecules into constituent atoms on the basis of the electron density (ρ). Minima, maxima and saddle points in the density critical points (CP), especially at the so-called bond critical points (BCPs), have found extensive use in characterizing bonding interactions, such as covalent,⁶⁰ hydrogen^{61,62} and π -stacking bonds.⁶³ Topologies were built using the *AIMPAC* series of programs.⁶⁴

Calculated Properties. To relate the structural changes of copper complexes occurring upon the redox process with their cleavage efficiency, the reorganization energy for Cu(phen)₂, Cu(2-Clip-phen), and Cu(3-Clip-phen) was estimated. According to Marcus theory, the rate of electron transfer is given by

$$k_{\text{ET}} = \frac{2\pi}{h} \frac{H_{\text{DA}}^2}{\sqrt{4\pi\lambda RT}} \exp\left(\frac{-(\Delta G^{\circ} + \lambda)^2}{4\lambda RT}\right) \quad (1)$$

where H_{DA} is the electronic coupling element that depends on the overlap between the wave functions of the two states, ΔG° is the free energy of the redox reaction, and λ is the so-called reorganization energy, i.e., the energy associated with the relaxing geometry of the system after electron transfer. In particular, for metal complexes, the inner-sphere reorganization energy (λ_{i}) is associated with the structural changes between reduced and oxidized forms, whereas the outer-sphere reorganization energy involves those associated with the solvent. λ_{i} is the sum of two contributions, λ_{red} and λ_{ox} , calculated as following: λ_{ox} as the difference between the energy of Cu(II) at its optimal geometry and the energy at the optimal geometry of the Cu(I) and λ_{red} as the difference between the energy of Cu(I) at its optimal geometry and the energy at the optimal geometry of the Cu(II) complex.^{65–69} Inner-sphere reorganization energies of coordination compounds are typically between 1 and 50 kcal/mol.^{65,68} Ionization energies (IE_{M}) for Cu-

- (42) Frisch, M. J. T.; G. W.; Schlegel, H. B.; Scuseria, G. E.; Robb, M. A.; Cheeseman, J. R.; Montgomery, Jr., J. A.; Vreven, T.; Kudin, K. N.; Burant, J. C.; Millam, J. M.; Iyengar, S. S.; Tomasi, J.; Barone, V.; Mennucci, B.; Cossi, M.; Scalmani, G.; Rega, N.; Petersson, G. A.; Nakatsuji, H.; Hada, M.; Ehara, M.; Toyota, K.; Fukuda, R.; Hasegawa, J.; Ishida, M.; Nakajima, T.; Honda, Y.; Kitao, O.; Nakai, H.; Klene, M.; Li, X.; Knox, J. E.; Hratchian, H. P.; Cross, J. B.; Adamo, C.; Jaramillo, J.; Gomperts, R.; Stratmann, R. E.; Yazyev, O.; Austin, A. J.; Cammi, R.; Pomelli, C.; Ochterski, J. W.; Ayala, P. Y.; Morokuma, K.; Voth, G. A.; Salvador, P.; Dannenberg, J. J.; Zakrzewski, V. G.; Dapprich, S.; Daniels, A. D.; Strain, M. C.; Farkas, O.; Malick, D. K.; Rabuck, A. D.; Raghavachari, K.; Foresman, J. B.; Ortiz, J. V.; Cui, Q.; Baboul, A. G.; Clifford, S.; Cioslowski, J.; Stefanov, B. B.; Liu, G.; Liashenko, A.; Piskorz, P.; Komaromi, I.; Martin, R. L.; Fox, D. J.; Keith, T.; Al-Laham, M. A.; Peng, C. Y.; Nanayakkara, A.; Challacombe, M.; Gill, P. M. W.; Johnson, B.; Chen, W.; Wong, M. W.; Gonzalez, C.; Pople, J. A. *Gaussian03*; Gaussian, Inc.: Pittsburgh PA, 2003.
- (43) Becke, A. D. *Phys. Rev. A* **1988**, 3098.
- (44) Lee, C. T.; Yang, W. T.; Parr, R. G. *Phys. Rev. B: Condens. Matter Mater. Phys.* **1988**, 37, 785–789.
- (45) Andrae, D.; Haussermann, U.; Dolg, M.; Stoll, H.; Preuss, H. *Theor. Chim. Acta* **1990**, 77, 123–141.
- (46) Cammi, R.; Mennucci, B.; Tomasi, J. *J. Phys. Chem. A* **2000**, 9100.
- (47) Becke, A. D. *J. Chem. Phys.* **1993**, 98, 5648–5652.
- (48) Boys, S. F.; Bernardi, F. *Mol. Phys.* **1970**, 19, 553.
- (49) Ghosh, A. *J. Biol. Inorg. Chem.* **2006**, 11, 712–724.
- (50) Stein, M.; Lubitz, W. *Phys. Chem. Chem. Phys.* **2001**, 3, 2668–2675.
- (51) Holland, J.; Green, J. C.; Dilworth, J. R. *Dalton Trans.* **2006**, 783–794.
- (52) Wang, X. J.; Wang, W.; Koyama, M.; Kubo, M.; Miyamoto, A. *J. Photochem. Photobiol., A* **2006**, 179, 149–155.
- (53) Atanasov, M.; Comba, P.; Martin, B.; Müller, V.; Rajaraman, G.; Rohwer, H.; Wunderlich, S. *J. Comput. Chem.* **2006**, 27, 1263–1277.

- (54) Perdew, J. P. *Phys. Rev. B: Condens. Matter Mater. Phys.* **1986**, 8822.
- (55) Burke, K.; Perdew, J. P.; Wang, Y. *Electronic Density Functional Theory: Recent Progress and New Directions*; Dobson, J. F., Vignale, G., Das, M. P., Eds.; Plenum: New York, 1998.
- (56) Moller, C.; Plesset, M. S. *Phys. Rev.* **1934**, 46, 618.
- (57) Bader, R. F. W. *Atoms in Molecules—A Quantum Theory*; Oxford University Press: Oxford, 1990.
- (58) Bader, R. F. W. *Chem. Rev.* **1991**, 91, 893–928.
- (59) Bader, R. F. W.; Essen, H. *J. Chem. Phys.* **1984**, 80, 1943–1960.
- (60) Howard, S. T.; Lamarche, O. *J. Phys. Org. Chem.* **2003**, 16, 133–141.
- (61) Boyd, R. J.; Choi, S. C. *Chem. Phys. Lett.* **1986**, 129, 62–65.
- (62) Grabowski, S. J. *Chem. Phys. Lett.* **2001**, 338, 361–366.
- (63) Waller, M. P.; Robertazzi, A.; Platts, J. A.; Hibbs, D. E.; Williams, P. A. *J. Comput. Chem.* **2006**, 27, 491–504.
- (64) Bieglerkonig, F. W.; Bader, R. F. W.; Tang, T. H. *J. Comput. Chem.* **1982**, 3, 317–328.
- (65) Amashukeli, X.; Gruhn, N. E.; Lichtenberger, D. L.; Winkler, J. R.; Gray, H. B. *J. Am. Chem. Soc.* **2004**, 126, 15566–15571.
- (66) Sigfridsson, E.; Olsson, M. H. M.; Ryde, U. *J. Phys. Chem. B* **2001**, 105, 5546–5552.
- (67) Olsson, M. H. M.; Ryde, U. *J. Am. Chem. Soc.* **2001**, 123, 7866–7876.
- (68) Ryde, U.; Olsson, M. H. M. *Int. J. Quantum Chem.* **2001**, 81, 335–347.
- (69) Parson, W. W.; Chu, Z. T.; Warshel, A. *Biophys. J.* **1998**, 74, 182–191.

(I)/Cu(II) couples were calculated as the energy difference between Cu(I) and Cu(II) species. According to equation 1, relative rates of electron transfer have been estimated assuming that $\Delta G \approx IE_{1/1}$ and that H_{DA} is unchanged for all the studied complexes.

Strain energies were calculated as the difference between the energy of Cu(phen)₂ at its own geometry and that of the Cu(phen)₂ fragment at the optimal geometry of corresponding clipped complexes. Formation energies of water adducts (ΔE_{H_2O}) were calculated via the supermolecule approach, i.e., $\Delta E_{H_2O} = E_{Cu(II)-H_2O} - (E_{Cu(II)} + E_{H_2O})$. All energies have been corrected by performing single-point calculations with an implicit solvent model (PCM)⁴⁶ on the geometries optimized in vacuo.

As in previous works,^{70,71} reduction potentials at standard conditions (E°) were estimated from the following equation

$$\Delta G^\circ = nFE^\circ \quad (1)$$

where $F = 96\,485\text{ C}$ (the Faraday constant), E° is the reduction potential, and n is the number of electrons involved in the redox process. Computed reduction potentials were referred to the normal hydrogen electrode, NHE. As shown in previous benchmark studies,⁷¹ DFT calculations with basis sets similar to those used in this work showed qualitative agreement with experimental results, with a virtual systematic error of $\sim 0.5\text{ V}$ between estimated and experimental reduction potentials. Large basis set and entropic corrections are required to drastically improve DFT performance.^{12,71} However, these corrections were not taken into account in this work since the main goal was to qualitatively describe the similarities and differences of the copper complexes studied.

To evaluate different DNA binding abilities of the reduced copper phenanthroline compounds, the program *Autodock 3.0* was employed,⁷² building an increasing number (N with $N = 10, 30, 50$) of complex/DNA adducts with each copper(I) species.

The DNA used was a double-strand 16mer, d[CGCTCAACT-GTGATAC]₂. This sequence was chosen as copper phenanthroline complexes preferably bind the pyrimidine-purine-pyrimidine triplet, such as TGT.^{25,73} The interactions between DNA and copper compounds were confined to the six central base pairs (reported in bold). Subsequently, statistical and energetic analysis was performed. Interaction energies of all the docked complexes are very similar ($\Delta E \approx 7\text{--}10\text{ kcal/mol}$), suggesting that most of the copper complex/DNA adducts are, in principle, possible. Results obtained with different values of N are equivalent; thus, only those corresponding to $N = 50$ were reported.

Results and Discussion

Structural Properties of Cu(phen)₂, Cu(2-Clip-phen), and Cu(3-Clip-phen). Test calculations confirmed that DFT-BLYP reproduces the structures of Cu(phen)₂⁺²⁺ and Cu(phen)₂(H₂O)²⁺ in good agreement with experimental data (see Supporting Information). Furthermore, geometries of clipped copper complexes optimized using the BLYP functional were compared to those obtained with B3LYP (Supporting Information).^{44,47} Also, the energies computed at B3LYP/6-311++G(2d,2p) are virtually equivalent to those obtained with BLYP/6-31+G(d,p), and, most importantly,

the energy trends of the clipped and unclipped complexes are maintained. These tests confirmed the accuracy of our computational scheme (Supporting Information).

In accordance with experimental^{74–77} and DFT^{38,40} studies, closed-shell Cu(phen)₂⁺ complexes slightly deviate from the D_{2d} symmetry. Structures minimized at BLYP/6-31G(d) present a dihedral angle (N1–N2–N3–N4, Figure 1) between the aromatic ligands equal to 81° , while the intraligand N1–Cu–N2 (Figures 1 and 2) and interligand N1–Cu–N3 angles are equal to 81° and 125° , respectively (Table 1). Cu–N bonds are virtually equivalent ($d \sim 2.08\text{ \AA}$) as confirmed by the AIM analysis (Supporting Information Figure 2S and Table 2) with electron densities at the Cu–N BCPs between 0.0691 and 0.0695 au. Interestingly, the oxidation process induces drastic changes on the copper coordination geometry and, in agreement with other studies,⁵² our calculations predict a more planar structure for Cu(phen)₂²⁺ with respect to Cu(phen)₂⁺ (Supporting Information, Figure 3S). The oxidized structure is also characterized by shorter Cu–N bonds (from $d = 2.08$ to 2.04 \AA), and a wider interligand N1–Cu–N3 angle (from 125° to 152°). In addition, the dihedral angle between aromatic rings of Cu(phen)₂²⁺ is markedly smaller than 90° (N1–N2–N3–N4 = 41°) (Figure 2 and Supporting Information Figure 3S), leading to shorter distances between the two H2 hydrogen atoms of opposite phenanthroline rings ($d = 2.65$ vs 4.63 \AA) with respect to Cu(phen)₂⁺. These geometrical features are mirrored in the AIM topology with Cu–N bonds presenting greater electron density at BCPs ($\rho \sim 0.0770\text{ au}$). In addition, new BCPs with $\rho \leq 0.005\text{ au}$ and new bond paths appear between the H2 hydrogen atoms, suggesting a small repulsive interaction (Supporting Information, Figure 2S).

It has been shown experimentally that Cu(II) complexes similar to those studied in this work are able of retaining their four-coordinated conformation in solution.⁷ Nevertheless, d⁹ cations undergo distortions resulting from the Jahn–Teller effect, and they usually are five- or distorted six-coordinated. Unfortunately, the exact nature of the DNA cleaving species is still unknown (Scheme 1).³ Since a large number of X-ray structures of water adducts of Cu(phen)₂ complexes is available (Supporting Information, Table 1S),⁷⁸ the effect of water as a fifth ligand was explored. In particular, the computed geometries of Cu(phen)₂(H₂O)²⁺ were compared to the available experimental data (see Supporting Information) as well as to those of the corresponding clipped complexes. Preliminary calculations were also performed on the complexes bearing a radical or anionic hydroxyl group as an apical ligand (see Supporting Informa-

(70) Blasco, S.; Demachy, I.; Jean, Y.; Lledos, A. *New. J. Chem.* **2001**, 25, 611–617.

(71) Baik, M. H.; Friesner, R. A. *J. Phys. Chem. A* **2002**, 106, 7407–7412.

(72) Garrett, M. M.; David, S. G.; Robert, S. H.; Ruth Huey, W.; Hart, E. R.; Belew, K.; Arthur, J. O. *J. Comput. Chem.* **1998**, 19, 1639–1662.

(73) Veal, J. M.; Rill, R. L. *Biochemistry* **1989**, 28, 3243–3250.

(74) Dobson, J. F.; Green, B. E.; Healy, P. C.; Kennard, C. H. L.; Pakawatchai, C.; White, A. H. *Aust. J. Chem.* **1984**, 37, 649–659.

(75) Blake, A. J.; Hill, S. J.; Hubberstey, P.; Li, W.-S. *J. Chem. Soc., Dalton Trans.* **1998**, 909–916.

(76) Hoffmann, S. K.; Corvan, P. J.; Singh, P.; Sethulekshmi, C. N.; Metzger, R. M.; Hatfield, W. E. *J. Am. Chem. Soc.* **1983**, 105, 4608–4617.

(77) King, G.; Gembicky, M.; Coppens, P. *Acta Crystallogr., Sect. C: Cryst. Struct. Commun.* **2005**, 61, M329–M332.

(78) Murphy, G.; Murphy, C.; Murphy, B.; Hathaway, B. *J. Chem. Soc., Dalton Trans.* **1997**, 2653–2600.

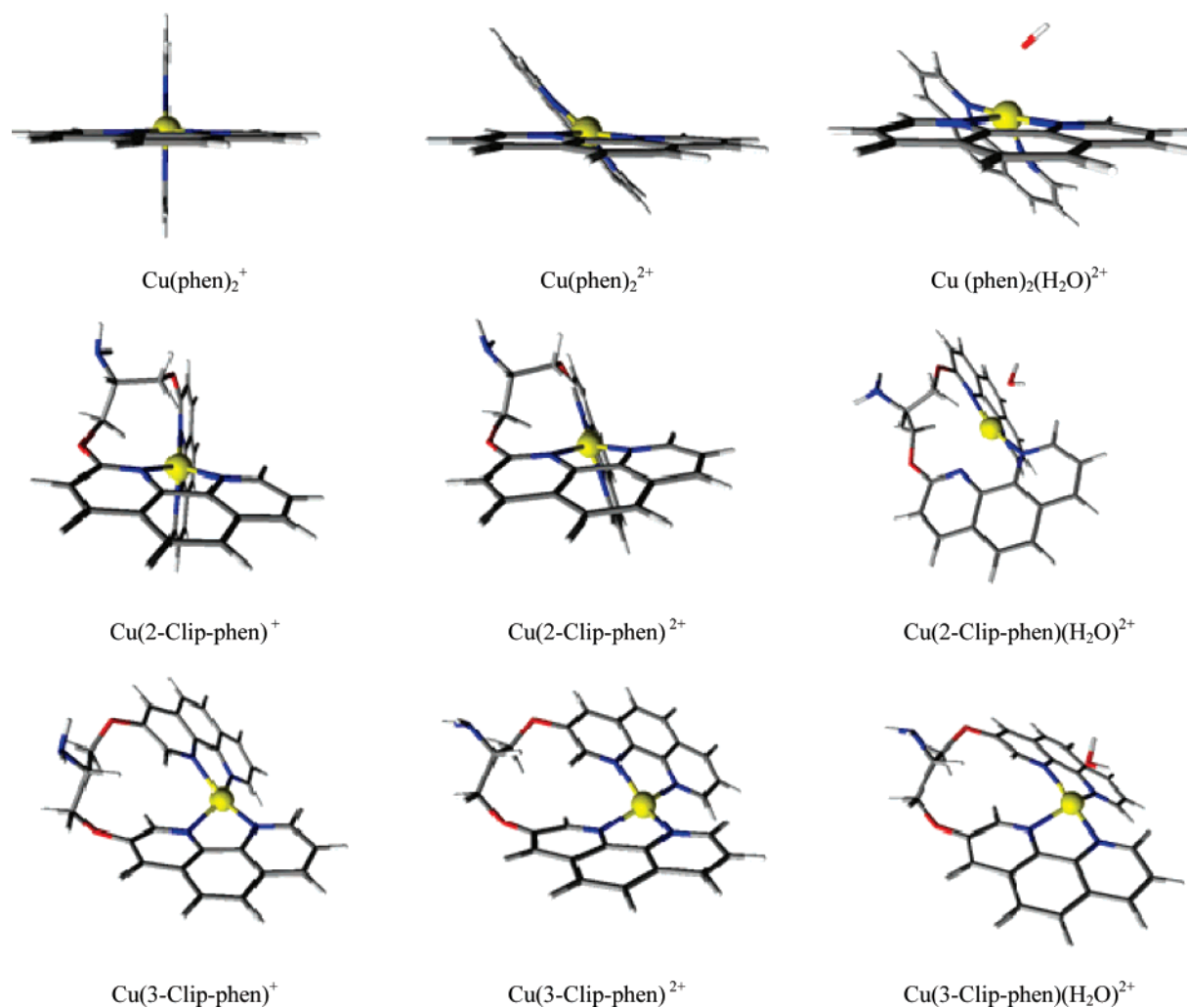


Figure 2. DFT-optimized structures of $\text{Cu}(\text{phen})_2^{+2+}$, $\text{Cu}(2\text{-Clip-phen})^{+2+}$, and $\text{Cu}(3\text{-Clip-phen})^{+2+}$ complexes. Complexes with a water molecule as the fifth coordination ligand are also depicted.

Table 1. Selected Bond Lengths (Å), Angles (deg), and Dihedral Angles (deg) of $\text{Cu}(\text{phen})_2^{+2+}$, $\text{Cu}(2\text{-Clip-phen})^{+2+}$, and $\text{Cu}(3\text{-Clip-phen})^{+2+}$. Structural Properties of Oxidized Complexes with a Water Ligand in the Apical Position are Also Given

oxidation state	ligand(s)	Cu–N1	Cu–N2	Cu–N3	Cu–N4	Cu–OH ₂	N1–Cu–N3	N1–N2–N3–N4
Cu(I)	(phen) ₂	2.07	2.07	2.08	2.08		125	81
	2-Clip-phen	2.16	2.05	2.04	2.17		125	82
	3-Clip-phen	2.14	2.07	2.06	2.14		146	49
Cu(II)	(phen) ₂	2.04	2.04	2.04	2.04		152	41
	2-Clip-phen	2.19	2.02	2.04	2.12		124	74
	3-Clip-phen	2.07	2.06	2.06	2.09		146	34
Cu(II)	(phen) ₂ (H ₂ O)	2.04	2.11	2.04	2.12	2.31	175	40
	(2-Clip-phen)(H ₂ O)	2.09	2.07	2.01	2.45	2.45	161	70
	(3-Clip-phen)(H ₂ O)	2.12	2.06	2.11	2.09	2.33	168	33

tion Tables 3S and 4S). However, a systematic study of the many hypotheses suggested by the experimental data^{1,3,31} is needed to identify the active cleaving species (Scheme 1).

The effect of water coordination is significant and leads to a distorted tetragonal symmetry (Table 1). Particularly, in agreement with previous DFT studies,⁴⁰ the binding of a water renders Cu–N bonds not equivalent (two shorter bonds of $d \sim 2.04$ Å and two longer bonds of $d \sim 2.12$ Å). The dihedral angle between phenanthroline rings becomes slightly smaller (40° vs 41° of $\text{Cu}(\text{phen})_2^{2+}$), while the N1–Cu–N3 angle increases sensibly, from 152° in $\text{Cu}(\text{phen})_2^{2+}$ to 175° (Figure 2). Moreover, the Cu–OH₂ bond length is 2.31 Å,

slightly longer than that seen in the experimental data (Table 1S). Interestingly, as the N1–N2–N3–N4 angle decreases, the distance between the H2 hydrogen atoms becomes even shorter than in $\text{Cu}(\text{phen})_2^{2+}$ (from 2.65 to 2.55 Å). The AIM topology of $\text{Cu}(\text{phen})_2(\text{H}_2\text{O})^{2+}$ confirms the formation of the Cu–OH₂ bond, showing a BCP between copper and water with an electron density equal to 0.0363 au (Table 2). Also, electron densities at BCP of Cu–N suggest the presence of two couples of equivalent bonds, $\rho \sim 0.0780$ and $\rho \sim 0.0650$ for shorter and longer bonds, respectively. Weak repulsive interactions are virtually unchanged from those of $\text{Cu}(\text{phen})_2^{2+}$.

Table 2. Electron Density and $\nabla^2\rho$ at Cu–N and Cu–OH₂ BCPs of Copper Phenanthroline Complexes

oxidation state	ligand(s)	Cu–N1		Cu–N2		Cu–N3		Cu–N4		Cu–OH ₂	
		ρ	$\nabla^2\rho$	ρ	$\nabla^2\rho$	ρ	$\nabla^2\rho$	ρ	$\nabla^2\rho$	ρ	$\nabla^2\rho$
Cu(I)	(phen) ₂	0.0691	0.0946	0.0692	0.0947	0.0694	0.0950	0.0695	0.0952		
	2-Clip–phen	0.0565	0.0700	0.0747	0.1030	0.0734	0.101	0.0578	0.0721		
	3-Clip–phen	0.0609	0.0750	0.0700	0.0957	0.0721	0.0984	0.0602	0.0756		
Cu(II)	(phen) ₂	0.0770	0.0939	0.0770	0.0939	0.0769	0.0939	0.0769	0.0940		
	2-Clip–phen	0.0643	0.0795	0.0777	0.0977	0.0807	0.1030	0.0544	0.0626		
	3-Clip–phen	0.0734	0.0895	0.0695	0.0849	0.0747	0.0913	0.0713	0.0865		
Cu(II)	(phen) ₂ (H ₂ O)	0.0774	0.928	0.0653	0.0786	0.0768	0.0927	0.0645	0.0778	0.0363	0.0397
	(2-Clip–phen)(H ₂ O)	0.0669	0.0810	0.0729	0.0894	0.0833	0.1030	0.0332	0.0254	0.0277	0.0227
	(3-Clip–phen)(H ₂ O)	0.0688	0.0828	0.0655	0.0794	0.0727	0.0873	0.0637	0.0770	0.0352	0.0367

Figure 2 displays structures of Cu(2-Clip–phen)⁺²⁺ and Cu(3-Clip–phen)⁺²⁺ optimized in the gas phase. The geometrical constraints imposed by the serinol bridge determine the opening of the binding angle and lead to two Cu–N types; i.e., Cu–N bonds closer to the 2 and 3 positions of phenanthroline (Cu–N1 and Cu–N4 in Figure 1) are longer, whereas those distant from the link (Cu–N3 and Cu–N2) are shorter. In particular, the Cu–N1 and Cu–N4 bonds of Cu(3-Clip–phen)₂⁺ are 2.14 Å long, whereas the Cu–N2 and Cu–N3 bonds are 2.06 Å long (Table 1). This behavior is mirrored in the electron density values at BCPs, $\rho \sim 0.0700$ and $\rho \sim 0.0600$ au for shorter and longer bonds, respectively. This trend is shown by all the tetracoordinated complexes.

Since species that effectively cleave DNA bear an additional ligand in the apical position, the structural features of five-coordinated complexes may also be very important to rationalize the cleavage activity of copper phenanthroline compounds. Interestingly, Cu(3-Clip–phen)(H₂O)₂²⁺ shows similar characteristics to Cu(phen)₂(H₂O)₂²⁺ (Figure 2). In particular, the Cu–N bonds differ by only ~ 0.06 Å on average and the Cu–OH₂ bond lengths are virtually equivalent ($\Delta d < 0.05$ Å), while the N1–Cu–N3 and N1–N2–N3–N4 angles differ by about 7°, on average. In contrast, the geometry of Cu(2-Clip–phen)(H₂O)₂²⁺ is rather distorted with the Cu–N4 bond significantly longer than the other C–N bonds (2.45 Å, compared with 2.01, 2.07, and 2.09 Å). Importantly, Cu(2-Clip–phen)(H₂O)₂²⁺ is not a global minimum of the potential energy surface. In fact, the geometry displayed in Figure 2 corresponds to a local minimum (chosen by monitoring forces acting on the structure), and it is reported only to show the structural distortions that Cu(2-Clip–phen)(H₂O)₂²⁺ undergoes with respect to the other water adducts.

The AIM topology analysis shows that the strength of the Cu–N4 bond decreases by $\sim 50\%$ after water coordination with $\rho \sim 0.0300$ au. In addition, the Cu–OH₂ bond is markedly longer than in Cu(phen)₂(H₂O)₂²⁺ and Cu(3-Clip–phen)(H₂O)₂²⁺ (2.45 Å vs 2.31 Å and 2.33 Å, respectively), and the electron density is 0.0277 au; i.e., the Cu–OH₂ bond is $\sim 30\%$ weaker than that of Cu(3-Clip–phen)(H₂O)₂²⁺. Interestingly, in vacuo full optimization of Cu(2-Clip–phen)(H₂O)₂²⁺ leads to a water adduct in which H₂O is not directly coordinated to the metal center, but the water shows a O \cdots H–C interaction with phenanthroline rings (Supporting Information, Figure 4S). In particular, the electron density

and its Laplacian at C–H \cdots O confirm the presence of a weak interaction, as $\rho = 0.0180$ au and $\nabla^2\rho = 0.0120$ au. Moreover, the N1–N2–N3–N4 dihedral angle is 70°, roughly 30° larger than those of Cu(phen)₂(H₂O)₂²⁺ and Cu(3-Clip–phen)₂(H₂O)₂²⁺.

Thus, the most intriguing structural parameters summarizing the geometrical differences among all studied complexes are the interligand N1–Cu–N3 angles and N1–N2–N3–N4 dihedral angles (Table 1). For instance, the N1–Cu–N3 angles range between 125° and 175° and 124° and 161° for Cu(phen)₂ and Cu(2-Clip–phen), respectively. This range is much narrower for Cu(3-Clip–phen), from 146° to 168°. Interestingly, the N1–N2–N3–N4 dihedral angles show a more pronounced dependence on the positions of the serinol link than on the oxidation states. For example, N1–N2–N3–N4 is 49°, 34°, and 33° for Cu(3-Clip–phen)⁺, Cu(3-Clip–phen)₂²⁺, and Cu(3-Clip–phen)(H₂O)₂²⁺, respectively, resembling the coordination geometries of Cu(phen)₂²⁺. At opposite, N1–N2–N3–N4 angles of the complexes bearing the 2-Clip–phen range between 82° and 70°, closer to that of Cu(phen)₂⁺.

Experimental studies point to a possible role played by Cu–hydroxyl species among several other putative active species (Scheme 1).^{2,3} Preliminary calculations on Cu(phen)₂, Cu(2-Clip–phen), and Cu(3-Clip–phen) complexes bearing an OH[–] or OH \cdot group as the fifth ligand were performed. In particular, while the coordination geometry is affected by the binding of the hydroxyl (anion and radical), the relative trend of the N1–N2–N3–N4 torsional angle is virtually retained (Supporting Information Tables 3S and 4S), leading to similar conclusions to those reported above.

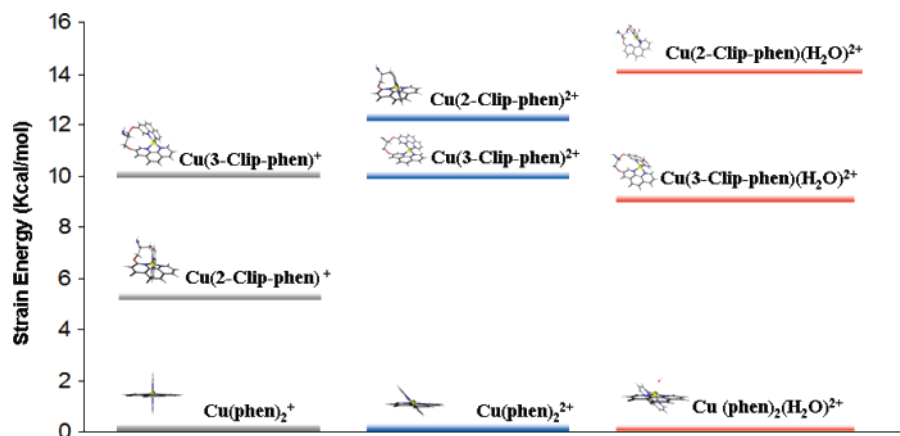
Energetics. Table 3 reports the relative energies of all studied complexes in both the gas phase and corrected with an implicit solvent model.⁴⁶ Ionization energies were calculated as reported in the Computational Details. To test the accuracy of the BLYP functional, we also performed single-point calculations of copper complexes in vacuo with different DFT functionals (such as B3LYP,^{44,47} BP,^{43,54} and PW91⁵⁵) (data not shown), using the same basis set as the one used for BLYP. The ionization energies calculated with different functionals hardly differ, demonstrating that the relative stabilities of reduced and oxidized complexes do not significantly depend on the functional used.

The IE_{I/II} of Cu(phen)₂^{+/}/Cu(phen)₂^{2+/} is ~ 207 kcal/mol, and it is reduced by ~ 100 kcal/mol in the presence of an implicit solvent model (IE_{I/II} ~ 109 kcal/mol). Clearly, the

Table 3. Energetic Profile (kcal/mol) and Reduction Potentials (V, vs NHE) of $\text{Cu}(\text{phen})_2^{+2+}$, $\text{Cu}(\text{2-Clip-phen})^{+2+}$, and $\text{Cu}(\text{3-Clip-phen})^{+2+}$ as well as $\text{Cu}(\text{phen})_2(\text{H}_2\text{O})^{2+}$, $\text{Cu}(\text{2-Clip-phen})(\text{H}_2\text{O})^{2+}$, and $\text{Cu}(\text{3-Clip-phen})(\text{H}_2\text{O})^{2+}$

	$\Delta E_{\text{H}_2\text{O}}^a$	strain energy			$\text{IE}_{\text{I/II}}^{b,c}$	E° (V, vs NHE)	$\lambda_{\text{red}}^{c,d}$	$\lambda_{\text{ox}}^{c,d}$	$\lambda_i^{c,d}$
		Cu(I)	Cu(II)	Cu(II)–H ₂ O					
(phen) ₂	36.0				206.8 (108.9)	0.29	9.0 (9.0)	10.0 (13.1)	19.0 (22.0)
(2-Clip-phen)	–	5.0	12.2	14.0	208.0 (119.3)	0.74	2.9 (3.4)	3.9 (2.5)	6.7 (5.9)
(3-Clip-phen)	35.0	11.0	10.0	9.0	202.4 (109.2)	0.31	5.2 (4.9)	6.2 (6.6)	11.4 (11.5)

^a Formation energies of water adducts. ^b $\text{IE}_{\text{I/II}}$ is calculated as $E_{\text{Cu(II)}} - E_{\text{Cu(I)}}$. ^c In parentheses are the energies calculated with the inclusion of the solvent. ^d See Computational Details for further information about λ_{red} , λ_{ox} , and λ_i .

**Figure 3.** Strain energies (kcal/mol) of $\text{Cu}(\text{2-Clip-phen})$ and $\text{Cu}(\text{3-Clip-phen})$ relative to those of the $\text{Cu}(\text{phen})_2$ complexes.

effect of solvent is larger for the oxidized complex, since the PCM takes into account mainly the electrostatic solute–solvent interactions. Clipped complexes show in vacuo energies similar to those of $\text{Cu}(\text{phen})_2$, with $\text{IE}_{\text{I/II}}$ slightly larger for $\text{Cu}(\text{2-Clip-phen})$ (~ 208 kcal/mol) and smaller for $\text{Cu}(\text{3-Clip-phen})$ (~ 202 kcal/mol). Interestingly, the $\text{IE}_{\text{I/II}}$ in a solution of $\text{Cu}(\text{3-Clip-phen})$ is virtually equivalent to that of $\text{Cu}(\text{phen})_2$ ($\Delta E < 1$ kcal/mol), while the $\text{IE}_{\text{I/II}}$ of the solvated complexes bearing a 2-Clip-phen link is larger ($\Delta E > 10$ kcal/mol) than those of previous ones. This scenario is mirrored in the copper complexes reduction potentials (E°) calculated as discussed in the Computational Details (Table 3). In particular, a very qualitative agreement exists between the calculated and experimental reduction potentials (measured on slightly different complexes from those studied in this work).²⁹ As suggested by experimental studies,²⁹ no clear correlation is found between the reduction potentials and cleavage activity of the clipped copper complexes.

The formation energy of water adducts ($\Delta E_{\text{H}_2\text{O}}$) of $\text{Cu}(\text{II})$ species was estimated to investigate the relative ability of clipped and nonclipped species to form five-coordinated complexes. $\Delta E_{\text{H}_2\text{O}}$ is ~ 36 and 35 kcal/mol for $\text{Cu}(\text{phen})_2(\text{H}_2\text{O})^{2+}$ and $\text{Cu}(\text{3-Clip-phen})(\text{H}_2\text{O})^{2+}$, respectively. In contrast, a direct comparison is not possible for $\text{Cu}(\text{2-Clip-phen})(\text{H}_2\text{O})^{2+}$, since in vacuo optimization leads to a complex with the water not directly coordinated to the metal center. This aspect, as well as the geometrical and topology properties discussed above, confirms that in the absence of DNA the formation of five-coordinated water complexes of $\text{Cu}(\text{2-Clip-phen})$ is not likely. This may be a significant drawback of copper phenanthroline complexes bearing a 2-Clip-phen link, assuming that the mechanism of DNA cleavage may proceed through the formation of five-

coordinated water intermediates.¹ Since it has been experimentally established that $\text{Cu}(\text{2-Clip-phen})$ is twice as reactive as $\text{Cu}(\text{phen})_2$, we cannot exclude that the relative ability to form a five-coordinated water complex may change in water solution and in the presence of the DNA. Furthermore, the exact nature of the reactive species responsible for the oxidative attack is unknown, and preliminary calculations on hydroxyl species indicate that five-coordinated complexes bearing a hydroxyl anion or radical may form for all clipped and unclipped structures (Supporting Information Tables 3S and 4S).

Strain energies (see Computational Details) reported in Table 3 and Figure 3 are important to rationalize the geometrical differences imposed by the serinol links. In particular, the strain energy of $\text{Cu}(\text{2-Clip-phen})^+$ is only 5 kcal/mol, confirming that the link induces no major structural changes with respect to $\text{Cu}(\text{phen})_2^+$. In contrast, the strain energy of $\text{Cu}(\text{3-Clip-phen})^+$ is ~ 11 kcal/mol, due to the significant geometrical differences discussed in the previous section. An opposite trend is observed for the oxidized species, for instance, $\text{Cu}(\text{2-Clip-phen})_2^{2+}$ and $\text{Cu}(\text{3-Clip-phen})_2^{2+}$ strain energies are 12 and 10 kcal/mol, respectively. Upon coordination of the fifth ligand, we observe that in $\text{Cu}(\text{3-Clip-phen})(\text{H}_2\text{O})^{2+}$ the strain energy is reduced by ~ 1 kcal/mol.

To estimate the effect of the serinol link on the redox properties of these copper complexes, inner-sphere reorganization energies were also calculated (see Computational Details). Table 3 displays the λ_{red} , λ_{ox} , and λ_i values of free and clipped copper phenanthroline complexes both in vacuo and in solution. The value of λ_i is 19 kcal/mol for $\text{Cu}(\text{phen})_2$ complexes, with contributions of 9 kcal/mol from λ_{red} and 10 kcal/mol from λ_{ox} . Solvation increases λ_{ox} by ~ 3 kcal/

mol, leading to a λ_i of 22 kcal/mol in solution. The serinol link is expected to reduce λ_i , since structural differences between the reduced and oxidized structures are less relevant. In particular, both λ_{ox} and λ_{red} of complexes with 3-Clip-phen are about 4 kcal/mol smaller than those of $\text{Cu}(\text{phen})_2$, with $\lambda_i \sim 11$ kcal/mol in vacuo. Likewise, λ_i is 7 kcal/mol for the complexes with 2-Clip-phen, since both λ_{red} and λ_{ox} decrease by ~ 6 kcal/mol. Unlike $\text{Cu}(\text{phen})_2$ complexes, the effect of solvent is marginal in the clipped structures ($\Delta E \leq 1.5$ kcal/mol). Thus, from equation 1 and the data displayed in Table 3, the redox properties of clipped complexes do not seem to correlate with their different abilities of cleaving DNA as already suggested experimentally by Pitić et al.²⁹

Copper Phenanthroline Complexes Binding to DNA. Relative Nuclease Efficiency. $\text{Cu}(3\text{-Clip-phen})$ reacts 60 times more efficiently than the unclipped complex, whereas $\text{Cu}(2\text{-Clip-phen})$ reacts only twice as much as $\text{Cu}(\text{phen})_2$.^{3,27,28} Experimental data²⁹ as well as our results suggest that differences in the relative DNA-cleavage efficiency of these complexes cannot be explained in terms of redox properties; thus, the geometrical features may play an important role in the DNA-cleavage activity.

Our studies clearly show that the serinol link has a crucial effect on the geometries of $\text{Cu}(2\text{-Clip-phen})^{+2+}$ and $\text{Cu}(3\text{-Clip-phen})^{+2+}$ complexes. In particular, the geometries of $\text{Cu}(2\text{-Clip-phen})^{+2+}$ hardly differ upon oxidation (i.e., the dihedral angle between phenanthroline rings is virtually constant) leading to structures always close to the $\text{Cu}(\text{phen})_2^{+2}$ geometry. In contrast, $\text{Cu}(3\text{-Clip-phen})^{+2+}$ complexes are fairly planar and similar to $\text{Cu}(\text{phen})_2^{+2}$. This point is significant, since the geometry differences may affect the way that phenanthroline compounds bind DNA, echoing the experimental findings of Pitić et al.²⁹ In particular, the mechanism of DNA cleavage is believed to occur through a partial intercalation and/or minor-groove binding of these complexes. Since planar molecules such as $\text{Cu}(3\text{-Clip-phen})$ should be favored for these binding modes, they are expected to cleave DNA more efficiently than nonplanar molecules, such as $\text{Cu}(\text{phen})_2$ and $\text{Cu}(2\text{-Clip-phen})$. Yet, the presence of the serinol link in clipped complexes favors the binding of two phen ligands. Indeed, copper complexes with two phen ligands cleave DNA more efficiently than those with only one phen.^{1,5–17} This may explain why $\text{Cu}(2\text{-Clip-phen})$ is more reactive than $\text{Cu}(\text{phen})_2$.

All these findings point to a major role of the structural properties for the cleavage activity of the copper phenanthroline complexes. The serinol link affects the structures of $\text{Cu}(2\text{-Clip-phen})$ and $\text{Cu}(3\text{-Clip-phen})$ complexes, modulating their DNA-cleavage activity.

Interaction with DNA Grooves and Intercalation. Since geometrical properties appear to be crucial in determining the binding mode of copper phenanthroline complexes to a double-strand oligonucleotide, docking simulations of $\text{Cu}(\text{phen})_2^{+2}$, $\text{Cu}(2\text{-Clip-phen})^{+2}$, and $\text{Cu}(3\text{-Clip-phen})^{+2}$ were performed to further investigate this aspect. For each $\text{Cu}(\text{I})$ complex, we built $N = 50$ (see Computational Details) adducts and evaluated their corresponding geometries. It should be stressed that these calculations were performed

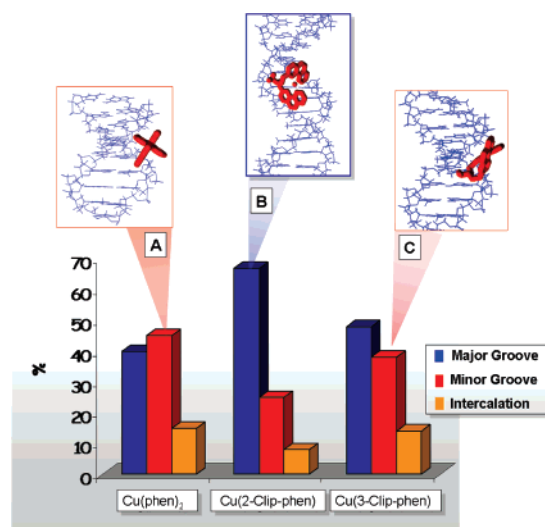


Figure 4. Probability of major-groove binding, minor-groove binding, and (partial) intercalation (%) for $\text{Cu}(\text{phen})_2^{+2}$, $\text{Cu}(2\text{-Clip-phen})^{+2}$, and $\text{Cu}(3\text{-Clip-phen})^{+2}$ adducts with a DNA oligomer d[CGCTCAACTGTGATAC] (see Computational Details for further information). Pictures represent the most stable adducts as determined by the *Autodock* software:⁷² (A) $\text{Cu}(\text{phen})_2^{+2}$, minor groove; (B) $\text{Cu}(2\text{-Clip-phen})^{+2}$, major groove; (C) $\text{Cu}(3\text{-Clip-phen})^{+2}$, minor groove.

keeping the conformations of both copper complexes and DNA fixed, while the binding is of course expected to induce geometrical rearrangements. Thus, these results are very qualitative, and they probably underestimate those binding modes (i.e., intercalation) that impose larger geometrical changes. Figure 4 summarizes these data in terms of the probability of (partial) intercalation, minor-groove binding, and major-groove binding for the three reduced complexes.

As mentioned above, experimental^{1,3,10,14,26} and theoretical^{34,35} studies focused on the binding modes of copper phenanthroline complexes with DNA. Several studies suggest that $\text{Cu}(\text{phen})_2$ preferably binds the DNA in the minor groove, with partial intercalation between base pairs. Data regarding clipped complexes are not as abundant as those of unclipped complexes, although their binding mode is believed to be similar.³

In agreement with these data,^{21,25,73,79,80} our results show that $\text{Cu}(\text{phen})_2^{+2}$ slightly prefers the minor groove ($\sim 45\%$) over the major groove ($\sim 40\%$), while a partial intercalation occurs with less probability ($\sim 15\%$). $\text{Cu}(3\text{-Clip-phen})^{+2}$ slightly prefers to bind to the major groove ($\sim 50\%$) over the minor groove ($\sim 40\%$), and a partial intercalation occurs with a probability of $\sim 10\%$. Nevertheless, the relative energies of the adducts indicate that in the most stable $\text{Cu}(3\text{-Clip-phen})^{+2}/\text{DNA}$ adduct, the copper complex lies in the minor groove, forming two strong hydrogen bonds, such as $\text{N}-\text{H}\cdots\text{O}$ (2.5 Å) and $\text{N}-\text{H}\cdots\text{N}$ (1.8 Å). This is remarkable, as experimental findings led to comparable conclusions.²⁹ In contrast, $\sim 70\%$ of the $\text{Cu}(2\text{-Clip-phen})^{+2}/\text{DNA}$ adducts appear to be located into the major groove, as the probability of minor-groove binding and intercalation is substantially smaller. Furthermore, the most stable $\text{Cu}(2\text{-Clip-phen})^{+2}/\text{DNA}$ adducts appear to be located into the major groove, as the probability of minor-groove binding and intercalation is substantially smaller.

(79) Veal, J. M.; Merchant, K.; Rill, R. L. *Nucleic Acids Res.* **1991**, *19*, 3383–3388.

(80) Veal, J. M.; Rill, R. L. *Biochemistry* **1991**, *30*, 1132–1140.

Clip-phen)⁺/DNA adduct shows the copper species into the major groove and no hydrogen bonds were detected. Within the approximation of this analysis, it is remarkable that Cu(phen)₂⁺ and Cu(3-Clip-phen)⁺ complexes can bind to DNA in several ways (including partial intercalation and minor-groove binding), whereas Cu(2-Clip-phen)⁺ mainly binds to the DNA in the major groove.

Summary and Conclusions

We have presented a theoretical study of Cu(phen)₂⁺²⁺, Cu(2-Clip-phen)⁺²⁺, and Cu(3-Clip-phen)⁺²⁺ complexes. Our results confirm that Cu(phen)₂⁺ undergoes significant geometrical changes upon oxidation to Cu(II), such as the strengthening of Cu-N bonds, the opening of interligand angles of N1-Cu-N3, and the reduction of dihedral angles between phenanthroline rings. In contrast, the geometries of Cu(2-Clip-phen)⁺²⁺ and Cu(3-Clip-phen)⁺²⁺ complexes depend more strongly on the position of serinol bridges than on their oxidation state, echoing experimental results.²⁹ For instance, the Cu(2-Clip-phen)⁺²⁺ geometry resembles that of Cu(phen)₂⁺, while the Cu(3-Clip-phen)₂⁺²⁺ structures are similar to Cu(phen)₂²⁺, retaining an almost planar arrangement of the phenanthroline rings.

Ionization energies for the three redox couples in the gas phase are rather similar, but they are affected differently by the inclusion of an implicit solvent model. Typically, the PCM model sensibly stabilizes Cu(II) species and leads to smaller IE_{I/II} energies. IE_{I/II} energies of solvated Cu(phen)₂⁺²⁺ and Cu(3-Clip-phen)₂⁺²⁺ differ by less than 2 kcal/mol, while IE_{I/II} for Cu(2-Clip-phen)⁺²⁺ is about 10 kcal/mol higher. Reorganization energies calculated for the three redox couples have the largest value in the Cu(phen)₂ (λ_i = 22.0 kcal/mol); this value decreases in Cu(3-Clip-phen) (λ_i = 11.5 kcal/mol) until a minimum value for Cu(2-Clip-phen) (λ_i = 5.9 kcal/mol) is reached. However, in agreement with experimental findings,²⁹ redox properties cannot account for the different DNA-cleavage efficiency of these compounds.

In contrast, the trend experimentally determined in the cleavage activity (3-Clip-phen ≫ 2-Clip-phen > Cu(phen)₂) may be attributed to the geometrical features of 3-Clip-phen and 2-Clip-phen. For instance, the former retains a certain planarity, ideal for intercalation or minor-groove binding, and the latter keeps the dihedral angle between aromatic rings larger than 70°, which may hamper such binding modes. Indeed, docking simulations show that Cu(phen)₂⁺ and Cu(3-Clip-phen)⁺ bind preferably in the minor groove, whereas Cu(2-Clip-phen)⁺ binds in the major groove.

In light of these results, the trend in cleavage activity Cu(3-Clip-phen) ≫ Cu(2-Clip-phen) > Cu(phen)₂ is only partly due to the increased affinity of copper for two phenanthroline rings caused by the serinol link. Indeed, the largest increase in the DNA-cleavage efficiency (i.e., Cu(3-Clip-phen) reacts 60 times more efficiently than Cu(2-Clip-phen)) may be ascribed to the planar structure of Cu(3-Clip-phen), which may bind DNA more strongly. Notably, our docking simulations showed the latter forming two hydrogen bonds in the minor groove, thereby stabilizing the interaction with DNA, in contrast to Cu(2-Clip-phen), which prefers the major groove.

In summary, our study provides an extensive electronic and structural characterization of copper phenanthroline compounds. This may be of interest for the design of novel mixed-metal anticancer complexes, where the unspecific copper phenanthroline ligand may be linked to sequence-selective anticancer compounds.³³

Supporting Information Available: Test calculations; Tables 1S and 2S contain a comparison between calculated and experimental geometrical parameters of copper complexes; Tables 3S and 4S report Cu-hydroxyl complexes bonding parameters; Figures 1S-4S. This material is available free of charge via the Internet at <http://pubs.acs.org>.

IC0618908